# Control of Sequence Distribution of Ethylene Copolymers: Influence of Comonomer Sequence on the Melting Behavior of Ethylene Copolymers

**Joyce Hung, Adam P. Cole, and Robert M. Waymouth***

*Department of Chemistry, Stanford University, Stanford, California 94305-5080*

*Received December 20, 2002*

ABSTRACT: New unbridged mixed-ligand zirconocenes were synthesized, characterized, and studied in the copolymerizations of ethylene−propylene (EP) and ethylene−1-hexene (EH). The MAO-activated metallocene [1-benzyl-2-(3′,5′-di-*tert*-butyl)phenylindenyl][2-phenylindenyl]zirconium dichloride (**8**) catalyzed EP and EH copolymerizations with products of reactivity ratios greater than one ($r_e r_p = 2.4$, $r_e r_h = 2.2$) to give rubbery, semicrystalline, high-melting polymers. Crystallinity was detected by differential scanning calorimetry (DSC) in both EP and EH copolymers containing only 50 mol % ethylene. Solvent fractionation of high ethylene content EH copolymers revealed that these copolymers were composed of a small ether-soluble fraction and heptane-soluble and heptane-insoluble fractions whose compositions and sequence distributions matched closely with those of the unfractionated polymer. Collectively, the reactivity ratios, DSC, and fractionation results gave evidence that these copolymers contained long crystallizable ethylene sequences. A comparison of the melting point behavior of a series of ethylene−1-hexene copolymers with 80 mol % ethylene revealed a sensitive dependence of the melting transition to the comonomer sequence distribution.

## Introduction

Metallocene catalysts for olefin polymerization have created new opportunities for the synthesis of polyolefins with defined and controlled microstructures.[1,2] One of the biggest impacts for these new classes of catalysts is in ethylene copolymers due to the ability of these catalyst systems to generate ethylene copolymers of uniform sequence and composition distributions. The copolymerization of ethylene with α-olefins is a common means of generating polyethylenes of controlled crystallinity and density. The introduction of short-chain branching derived from the comonomer decreases the crystallinity and melting temperature of copolymer as the co-units interfere with crystallization and reduce the size of crystallites. It is well-known that randomly introduced comonomer units cause a decrease in both the density and in the melting temperature of ethylene-α-olefin copolymers.[3−9] This melting point depression in random copolymers, where the co-unit is completely excluded from the crystal lattice, has been described by Flory's copolymer melting equation:

$$\frac{1}{T_m} - \frac{1}{T_m{}^0} = -\frac{R}{\Delta H_u} \ln p \qquad (1)$$

where $T_m$ and $T_m{}^0$ are the melting temperatures of the copolymer and homopolymer, respectively, $R$ is the gas constant, $\Delta H_u$ is the enthalpy of fusion per repeating unit, and $p$ is the probability that a randomly added crystallizable unit is followed by another such unit.[10] For random copolymers, the parameter $p$ is related to the mole fraction of crystallizable units. However, as pointed out by both Flory and Allegra, the parameter $p$ will also depend on the sequence distribution.[8,10] At any given composition, the melting temperature of a block copolymer will be the highest, that of an alternating copolymer will be the lowest, and that of a random copolymer will be somewhere in between. Thus, while the introduction of comonomers will typically lower the density, the magnitude of the melting point depression depends sensitively on both the composition and sequence distribution of the comonomer.

While the impact of sequence distribution on the melting properties of ethylene copolymers has been long appreciated, there are currently no general synthetic strategies for the catalytic synthesis of ethylene copolymers of a predefined and controlled sequence distribution.[11−15] Recently, we and several other groups have begun to investigate strategies for controlling the sequence distributions in olefin copolymers.[13,14,16−25] In this manuscript, we describe the synthesis and polymerization behavior of a family of unbridged metallocenes that yield ethylene copolymers with a range of different sequence distributions. One of these catalyst systems yields semicrystalline ethylene−propylene and ethylene−1-hexene copolymers with high melting points and a sequence distribution ($r_e r_p = 2.4$ and $r_e r_h = 2.2$) that leads to long crystallizable ethylene sequences. A comparison of the melting point behavior of a series of ethylene−1-hexene copolymers with 80 mol % ethylene revealed a sensitive dependence of the melting transition to the comonomer sequence distribution.

## Results

**Synthesis of Mixed-Ligand Complexes.** For this study, two mixed-ligand zirconium dichloride complexes were prepared in a two-step procedure as previously described (eq 2).[26] The reactions proceeded in good

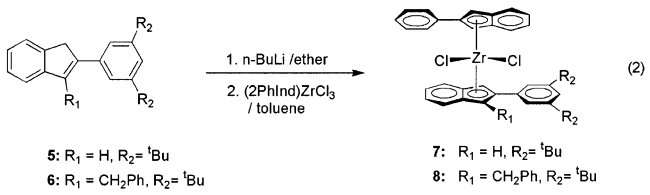


**5:** $R_1$ = H, $R_2$ = $^t$Bu
**6:** $R_1$ = $CH_2Ph$, $R_2$ = $^t$Bu
**7:** $R_1$ = H, $R_2$ = $^t$Bu
**8:** $R_1$ = $CH_2Ph$, $R_2$ = $^t$Bu

(2)

yield, but the metallocenes [2-(3′,5′-di-*tert*-butyl)phenylindenyl][2−phenylindenyl]zirconium dichloride (**7**) and [1-benzyl-2-(3′,5′-di-*tert*-butyl)phenylindenyl][2-phenylindenyl]zirconium dichloride (**8**) were isolated in low

10.1021/ma021779v CCC: $25.00 © 2003 American Chemical Society
Published on Web 03/11/2003

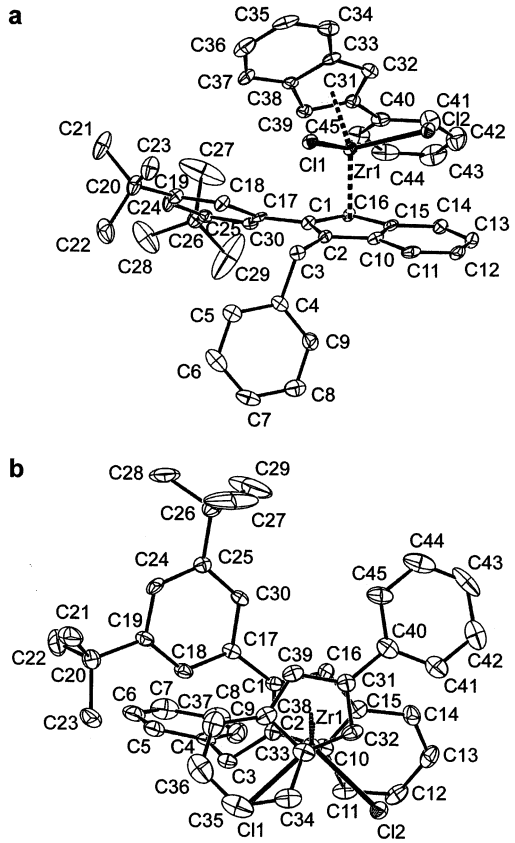


**Figure 1.** X-ray crystal structure of mixed-ligand metallocene **8**: (a) front view; (b) top view, "crisscross" conformation.

**Table 1. Selected Bond Angles and Distances for [1-Benzyl-2-(3′,5′-di-*tert*-butyl)phenylindenyl]-[2-phenylindenyl]zirconium Dichloride (8)**

| defining atoms[a] | bond distances in Å and bond angles in deg |
|---|---|
| Zr(1)−Cg(1) | 2.251 |
| Zr(1)−Cg(2) | 2.238 |
| Zr(1)−Cl(1) | 2.422 |
| Zr(1)−Cl(2) | 2.430 |
| C(1)−C(17) | 1.469 |
| C(31)−C(40) | 1.477 |
| Cg(1)−Zr(1)−Cg(2) | 131.26 |
| Cl(1)−Zr(1)−Cl(2) | 94.06 |
| plane 1/plane 2 | 22.27(3) |
| plane 3/plane 4 | 27.89(3) |

[a] Cg(1) = 1-benzyl-2-phenylindenyl centroid. Cg(2) = 2-phenylindenyl centroid. Plane 1 = C(31), C(32), C(33), C(38), C(39). Plane 2 = C(40), C(41), C(42), C(43), C(44), C(45). Plane 3 = C(1), C(2), C(10), C(15), C(16). Plane 4 = C(17), C(18), C(19), C(24), C(25), C(30).

yields due to their high solubility. The 1-benzyl mixed-ligand complex **8** exhibited two distinct doublets ($^2J_{HH}$ = 16−17 Hz) in the $\delta$ 4.6−4.8 ppm region of the $^1$H NMR spectrum, which corresponded to the diastereotopic benzyl protons, as well as characteristic doublet−doublet−singlet peaks in the cyclopentadienyl proton region, typical for 1-substituted mixed-ligand complexes.

Orange crystals of **8**, suitable for X-ray diffraction analysis, were grown by slow evaporation from a saturated heptane/toluene solution of the complex. The X-ray crystal structure of **8** is shown in Figure 1, and some selected bond lengths and angles are listed in Table 1. The complex adopted a crisscross conformation in the solid state, as shown in Figure 2b. Aside from the somewhat larger dihedral angles between the phenyl and indenyl rings (22.27 and 27.89°), most other angles and distances were similar to those of bis(2-phenylindenyl)zirconium dichloride (**2**).[27]

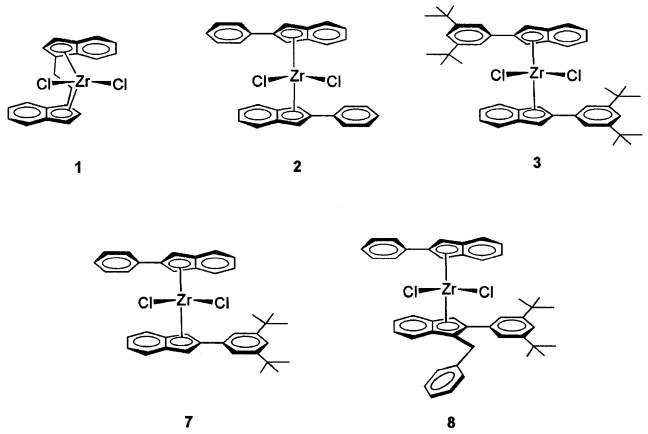


**Figure 2.** Structures of metallocenes **1**, **2**, **3**, **7**, and **8**.

**Polymerization Behavior.** The polymerization behavior of a variety of metallocenes was investigated and compared to that of metallocenes **7** and **8** (Figure 2). Propylene homopolymerizations were carried out in liquid propylene with metallocenes bis(2-phenylindenyl)zirconium dichloride (**2**/MAO) and bis(2-(3′,5′-di-*tert*-butyl)phenylindenyl)zirconium dichloride (**3**/MAO), and the mixed-ligand metallocenes **7**/MAO and **8**/MAO.[28] As previously reported,[29] the bis(2-(3′,5′-di-*tert*-butyl)-phenylindenyl)zirconium dichloride (**3**) has a similar productivity but yields a much more highly isotactic polypropylene ([mmmm] = 80%) than the unsubstituted metallocene **2** ([mmmm] = 28%). In contrast, the mixed-ligand compound **7**, containing only one *tert*-butyl-substituted ligand has a productivity similar to that of **2** and also yields a polypropylene of similar microstructure ([mmmm] = 34%). Introduction of a benzyl substituent on the cyclopentadienyl ring to give **8** yields a catalyst with a significantly lower productivity than those generated from **2**/MAO, **3**/MAO, and **7**/MAO; nevertheless, the polymer produced has a slightly less tactic microstructure ([mmmm] = 24%) than that produced from **2**/MAO.

Ethylene−propylene (EP) copolymerizations were carried out with **2**/MAO, **3**/MAO, **7**/MAO, and **8**/MAO and were compared to that of *rac*-[ethylenebis(1-indenyl)]zirconium dichloride (*rac*-EBIZrCl$_2$, **1**) (Tables 2 and 3). Copolymerizations with **8**/MAO resulted in lower molecular weight EP copolymers and productivities that were 2 orders of magnitude lower than those obtained from **2**/MAO,[30] **3**/MAO, and **7**/MAO. For similar ethylene−propylene feed ratios ($X_e/X_p$ = 0.13−0.16), the productivities and molecular weights increased in the order **8**/MAO ≪ **2**/MAO ∼ **7**/MAO < **3**/MAO. The polymerization behavior of **2**/MAO and **7**/MAO were similar. While the polydispersities were reasonably narrow for both **3**/MAO (PDI = 2.4) and **7**/MAO (PDI = 2.7), they were somewhat broad for **8**/MAO (PDI = 3.2). As observed with propylene polymerization, the 1-benzyl group depressed the catalyst activity and polymer molecular weight, while the presence of 3′,5′-di-*tert*-butyl groups on *both* 2-phenylindenyl ligands led to higher catalyst activity and EP copolymers with higher molecular weight.

Ethylene−1-hexene (EH) copolymerizations were conducted with **8**/MAO to determine the influence of the α-olefin on the copolymerization behavior and polymer

**Table 2. Ethylene−Propylene Copolymerizations with 1/MAO, 2/MAO, 3/MAO, and 7/MAO**

| sample | catalyst | % E [a] | $X_e/X_p$ [b] | $r_e$ [c] | $r_p$ [c] | $r_e r_p$ [c] | productivity (kg/mol·Zr·h) | $T_m$ [d] (°C) | $\Delta H_f$ [d] (J/g) | $M_w$ [e] ($\times 10^{-3}$) | PDI[e] |
|---|---|---|---|---|---|---|---|---|---|---|---|
| 1 | **1**/MAO | 63 | 0.15 | 9.7 | 0.05 | 0.5 | 19 200 | | | | |
| 2 | **2**/MAO | 30 | 0.13 | 3.19 | 0.26 | 0.84 | 145 000 | none | none | | |
| 3 | **3**/MAO | 18 | 0.10 | 2.36 | 0.45 | 1.1 | 205 000 | 30−65 (46, 58) | 1.4 | 2317 | 2.4 |
| 4 | | 26 | 0.15 | 2.62 | 0.41 | 1.1 | 527 000 | none | none | | |
| 5 | **7**/MAO | 20 | 0.09 | 3.14 | 0.36 | 1.1 | 76 300 | | | | |
| 6 | | 31 | 0.16 | 3.06 | 0.32 | 0.96 | 180 000 | none | none | 1385 | 2.7 |

[a] Mole % ethylene in the polymer, determined by $^{13}C$ NMR. [b] Ratio of mole fractions of ethylene and propylene in the feed. [c] Reactivity ratios of ethylene ($r_e$), propylene ($r_p$), and their product ($r_e r_p$), determined by $^{13}C$ NMR. [d] Determined by DSC. Numbers in parentheses are peak melting temperatures. [e] Determined by GPC (BP Amoco).

**Table 3. Ethylene−Propylene Copolymerizations with 8/MAO**

| sample | % E [a] | $X_e/X_p$ [b] | $r_e$ [c] | $r_p$ [c] | $r_e r_p$ [c] | productivity (kg/mol·Zr·h) | $T_m$ [d] (°C) | $\Delta H_f$ [d] (J/g) | $M_w$ [e] ($\times 10^{-3}$) | PDI[e] |
|---|---|---|---|---|---|---|---|---|---|---|
| 7 | 0 | | | | | 310 | 30−155 (135) | 17.4 | 73.1 | 2.9 |
| 8 | 40 | 0.08 | 13.7 | 0.18 | 2.5 | 1900 | 35−60 (45) | 2.1 | | |
| 9 | 45 | 0.11 | 12.2 | 0.19 | 2.3 | 1000 | 35−80 (49) | 5.2 | | |
| 10 | 50 | 0.13 | 12.7 | 0.18 | 2.2 | 2400 | 35−80 (71) | 6.2 | 343 | 3.2 |
| 11 | 55 | 0.15 | 12.9 | 0.18 | 2.3 | 4600 | 35−90 (78) | 7.6 | | |
| 12 | 60 | 0.18 | 12.1 | 0.18 | 2.2 | 7900 | 35−95 (84) | 8.0 | 401[f] | 2.8[f] |
| 13 | 100 | | | | | 3500 | 139 | 163 | 780 | 4.6 |
| optimized[g] | | | $r_e = 12.1 \pm 0.9$ | | | | $r_p = 0.19 \pm 0.02$ | | | $r_e r_p = 2.4 \pm 0.3$ |

[a] Mole % ethylene (% E) in the polymer, determined by $^{13}C$ NMR. [b] Ratio of mole fractions of ethylene and propylene in the feed. [c] Reactivity ratios of ethylene ($r_e$), propylene ($r_p$), and their product ($r_e r_p$), determined by $^{13}C$ NMR. [d] Determined by DSC. Numbers in parentheses are peak melting temperatures. [e] Determined by GPC (BP Amoco). [f] Determined by DuPont Dow Elastomers. [g] Using Microsoft Excel Solver, optimized values for $r_e$ and $r_p$ were obtained from a least squares minimization of the difference between experimental and theoretical triad distribution based on a first-order Markovian model for copolymerization.

**Table 4. Ethylene-1-Hexene Copolymerizations with 8/MAO**

| sample | % E [a] | $X_e/X_h$[b] | $r_e$ [c] | $r_h$ [c] | $r_e r_h$ [c] | productivity (kg/mol·Zr·h) | $T_m$ [d] (°C) | $\Delta H_f$ [d] (J/g) | $M_w$ [e] ($\times 10^{-3}$) | PDI[e] |
|---|---|---|---|---|---|---|---|---|---|---|
| 14 | 49 | 0.06 | 22.2 | 0.08 | 1.8 | 1260 | 30−65 (42) | 0.9 | 135 | 4.1 |
| 15 | 61 | 0.08 | 26.3 | 0.07 | 1.9 | 2100 | 28−80 (39) | 5.2 | 214 | 3.8 |
| 16 | 68 | 0.11 | 24.7 | 0.08 | 1.8 | 2380 | 25−90 (36, 73) | 10.7 | 278 | 3.6 |
| 17 | 72 | 0.15 | 23.2 | 0.08 | 1.9 | 4160 | 25−95 (36, 79) | 14.2 | | |
| 18 | 75 | 0.18 | 20.1 | 0.09 | 1.8 | 7800 | 25−100 (37, 86) | 18.7 | 562 | 4.0 |
| 19 | 80 | 0.23 | 20.2 | 0.09 | 1.8 | 11 900 | 28−104 (37, 89) | 18.0 | | |
| 20 | 84 | 0.28 | 20.4 | 0.09 | 1.8 | 14 800 | 28−105 (37, 93) | 21.4 | | |
| 21 | 85 | 0.31 | 19.9 | 0.10 | 2.0 | 16 100 | 28−106 (37, 94) | 23.2 | 630 | 3.9 |
| optimized[f] | | | $r_e = 25 \pm 4$ | | | | $r_h = 0.09 \pm 0.01$ | | | $r_e r_h = 2.2 \pm 0.4$ |

[a] Mole % ethylene in the polymer, determined by $^{13}C$ NMR. [b] Ratio of mole fractions of ethylene and 1-hexene in the feed. [c] Reactivity ratios of ethylene ($r_e$), propylene ($r_h$), and their product ($r_e r_h$), determined by $^{13}C$ NMR. [d] Determined by DSC. Samples aged for 36 h. Numbers in parentheses are peak melting temperatures. [e] Determined by GPC (BP Amoco). [f] Using Microsoft Excel Solver, optimized values for $r_e$ and $r_h$ were obtained from a least squares minimization of the difference between experimental and theoretical triad distribution based on a first-order Markovian model for copolymerization.

properties (Table 4). Both productivity and molecular weight increased with increasing ethylene in the feed. The catalyst productivities and molecular weights of both EP and EH copolymers were very close for similar ethylene feeds. However, for any given ethylene/comonomer feed ratio, more ethylene was incorporated into the EH copolymers than was incorporated into the EP copolymers. The polydispersities of the EH copolymers were slightly broader (PDI = 3.6−4.8) than those of the EP copolymers.

**Reactivity Ratios for Ethylene—α-Olefin Copolymerization.** The triad distributions and reactivity ratios ($r_e$, $r_c$ as reported in Tables 2−5) for all copolymerization catalyst systems were calculated from individual $^{13}C$ NMR spectra of the resulting copolymers using Kakugo's method and Randall's peak assignments for EP and EH copolymers.[31−33] Optimized values of $r_e$ and $r_c$ used to report the overall $r_e r_c$ for both EP and EH copolymerizations with **8**/MAO (bottom, Tables 3 and 4) were obtained from a first-order Markovian fit of the experimental data from individual runs. This was done using Microsoft Excel solver, which optimized values for $r_e$ and $r_c$ by a least-squares minimization of the difference between experimental and theoretical triad distributions. Standard error propagation methods were used to obtain the reported error values.[34]

Reactivity ratio results for the widely studied *rac*-EBIZrCl$_2$ **1**/MAO were included for comparison with literature data (Table 2). The reactivity ratios for ethylene and propylene ($r_e = 9.7$, $r_p = 0.05$) correlated well with literature values, to give a product of reactivity ratios of $r_e r_p = 0.5$.[20,30,35−38]

The low calculated values of $r_e$ = 2.4−3.2, and relatively high values of $r_p$ = 0.26−0.45 indicate that the unbridged metallocenes **2**, **3**, **7**, and **8** are very efficient in incorporating comonomer, even better than the *ansa*-metallocene **1** (Table 2). The ethylene−propylene triad sequence distributions for copolymers of similar ethylene content made from **2**/MAO, **3**/MAO, and **7**/MAO were similar, as manifested both by analysis of the sequences (see Supporting Information for sequence distributions) and by the calculated $r_e r_p$ = 0.84−

**Table 5. Temperature Dependence of Ethylene-1-Hexene Copolymerizations with 8/MAO**

| sample | $T_{pol}$ [a] (°C) | % E [b] | $X_e/X_h$ [c] | $r_e$ [d] | $r_h$ [d] | $r_e r_h$ [d] | productivity (kg/mol·Zr·h) | $T_m$ [e] (°C) | $\Delta H$ [e] (J/g) | $M_w$ [f] ($\times 10^{-3}$) | PDI [f] |
|---|---|---|---|---|---|---|---|---|---|---|---|
| 22 | 2 | 82 | 0.313 | 17.2 | 0.12 | 2.1 | 20 100 | 30−109 (42,96) | 15.3 | 1142 | 2.4 |
| 23 | 20 | 85 | 0.303 | 22 | 0.11 | 2.4 | 7900 | 30−111 (42,96) | 26.4 | 615 | 2.5 |
| 24 | 50 | 84 | 0.215 | 25 | 0.05 | 1.2 | 760 | 31−105 (43,90) | 13.3 | 232 | 3.2 |

[a] Polymerization temperature. [b] Mole % ethylene in the polymer, determined by $^{13}C$ NMR. [c] Ratio of mole fractions of ethylene and 1-hexene in the feed. [d] Reactivity ratios of ethylene ($r_e$), 1-hexene ($r_h$), and their product ($r_e r_h$), determined by $^{13}C$ NMR. [e] Determined by DSC. Numbers in parentheses are peak melting temperatures. [f] Determined by GPC at DuPont Dow Elastomers.

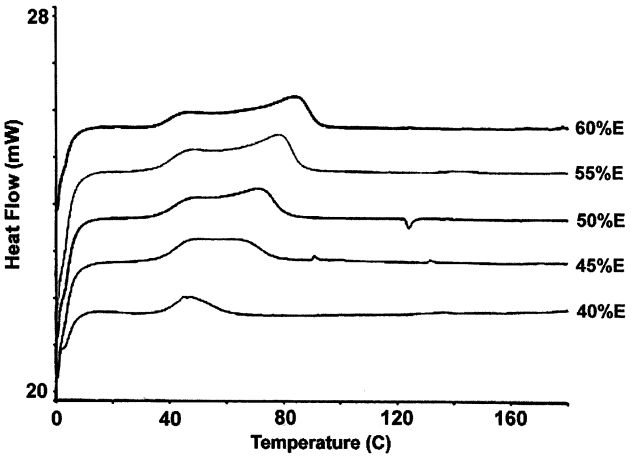


**Figure 3.** DSC heating curves for ethylene−propylene copolymers made from **8**/MAO. Bottom to top: increasing ethylene content in copolymers (40−60%).

1.1 range, which spans the value $r_e r_p = 1$ indicative of a random copolymer. In contrast, the sequence distributions for copolymers derived from **8**/MAO showed enhancements in the PPP and EEE triads that were approximately twice that observed in EP copolymers prepared from **2**/MAO, **3**/MAO, or **7**/MAO at similar compositions. This is also manifested in the higher $r_e r_p = 2.2-2.5$ calculated for **8** relative to those calculated for **2**/MAO, **3**/MAO, or **7**/MAO. These data indicate that the copolymers derived from **8** contain longer ethylene sequences than those derived from **1**, **2**, **3**, or **7**. Similar trends are observed in the ethylene−1-hexene copolymers: the ethylene−1-hexene copolymers derived from **8** contain longer ethylene homosequences than expected for a random copolymer.

**Temperature Dependence of Ethylene—1-Hexene Copolymerizations with 8/MAO.** For EH copolymerizations with **8**/MAO, the productivity was greatest at lower temperatures and decreased by 2 orders of magnitude as the polymerization temperature was increased from 2 to 50 °C (Table 5). The molecular weight also decreased significantly with increasing temperature. The reactivity $r_e$ increased with increasing temperature while $r_h$ decreased with increasing temperature such that $r_e r_h$ at 50 °C was closer to 1. The increase in polydispersity and decrease in productivity as the polymerization temperature was increased to 50 °C is consistent with the decomposition of the catalyst at higher polymerization temperatures. For similar ethylene contents (82−85%), the EH copolymer produced at 20 °C was the highest melting and most crystalline.

**Thermal Properties.** The differential scanning calorimetry (DSC) heating curves for EP and EH copolymers made by **8**/MAO are shown in Figures 3 and 4. Melting ranges and enthalpies of fusion are listed in Tables 3 and 4. The amount of crystallinity, as well as the maximum melting temperature, increased with ethylene content. The presence of a small amount of crystallinity in both EP and EH copolymers containing 40 and 50% ethylene, respectively, provided additional indications of ethylene sequences long enough to crystallize even at close to 1:1 ratios of monomer units in the polymer. The higher melting temperature of EP copolymers of similar composition to EH copolymers could be attributed to the cocrystallization of propylene units with polyethylene sequences.

The melting endotherms of a series of isothermally crystallized high ethylene content EH copolymers made by **8**/MAO (Figure 5) appeared to be very similar in profile to those of ethylene-1-octene (EO) copolymers made using Dow's INSITE constrained geometry catalyst technology (CGCT).[39] However, as expected, the EH copolymers exhibited higher melting temperatures at higher comonomer content, reflecting the presence of longer ethylene sequences in the copolymers made by **8**/MAO. The broad melting ranges observed in copolymers made by both CGCT and **8**/MAO indicated a distribution of crystallite sizes—a consequence of the range of different ethylene sequence lengths in the copolymers. The crystallization behavior of ethylene copolymers made by these single-site catalysts seemed to produce two different populations of crystal types (or sizes), one of which was associated with the lower melting endotherm and the other with the higher melting endotherm.[39−41] The lower melting endotherm systematically moved to higher temperatures with increasing annealing temperature, as thinner crytals could melt and recrystallize into thicker crystals; however, the higher melting endotherm, present only in copolymer samples with ethylene sequences long enough to form larger crystals, did not change significantly with increasing annealing temperatures. The enthalpy of fusion remained constant with different annealing temperatures, indicating that the same population of ethylene sequences crystallized at each annealing temperature even though the crystal sizes and types may vary. The total enthalpy of fusion and the temperature at which the high melting peak appeared could be directly correlated to the comonomer content in the copolymer.

For the copolymers with the highest comonomer content (40−50% ethylene), the absence of the high melting endotherm could be attributed to the lack of ethylene sequences long enough to form thicker, higher-melting crystals. However, these shorter ethylene sequences were able to associate to form smaller crystallites which were manifested by the low melting endotherm. As seen in copolymers made by CGCT, the presence of shorter ethylene sequences even in high ethylene content copolymers could account for the multimodal nature of the DSC melting traces for copolymers made by **8**/MAO.

**Fractionations of Ethylene—1-Hexene Copolymer.** Fractionations were carried out to determine the composition distribution of the EH copolymers. Several

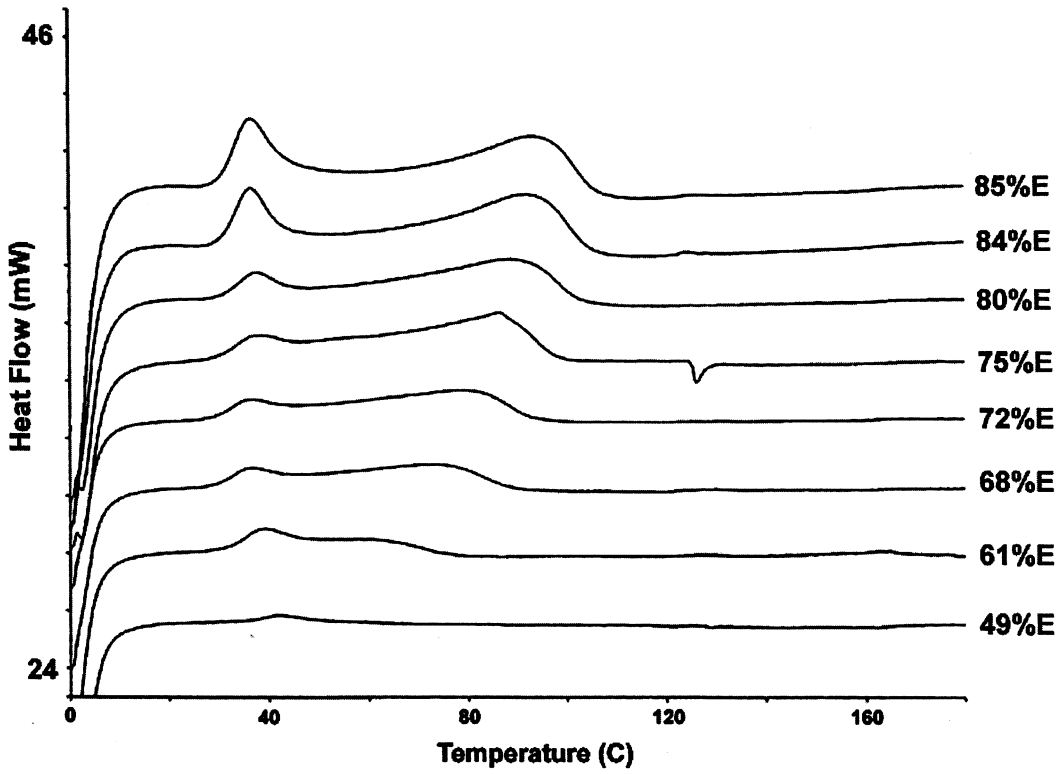


**Figure 4.** DSC heating curves for ethylene−1-hexene copolymers made from **8**/MAO. Bottom to top: increasing ethylene content in copolymers (49−85%).

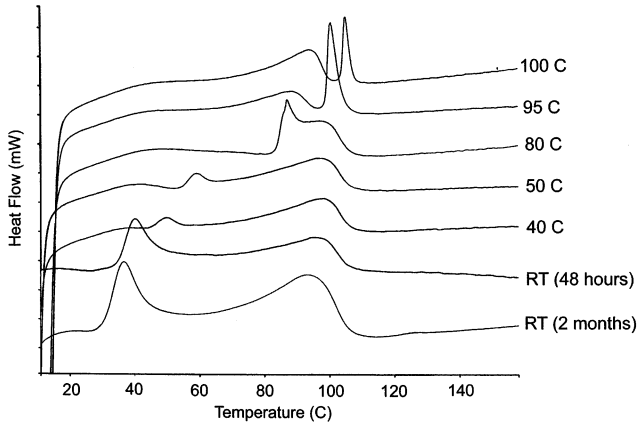


**Figure 5.** DSC melting endotherms for a series of isothermally crystallized EH copolymers made by **8**/MAO (85% ethylene). Annealing temperatures are indicated on the right.

high ethylene content EH copolymers made from **8**/MAO were fractionated by successive extractions into refluxing ether and then heptane for 24 h each in a Kumagawa extractor under nitrogen; the results from one of these fractionations is given in Table 6.

DSC melting curves for an ethylene−1-hexene copolymer of 84 mol % ethylene and its fractions are shown in Figure 6. For a series of five copolymers, the ether-soluble (ES) fractions differed from the heptane-soluble (HS) and heptane-insoluble (HI) fractions (see Supporting Information for fractionation data). In every sample, the ES fraction constituted less than 10% weight of the whole polymer, contained consistently around 70% ethylene random copolymer, and was lower in molecular weight, lower in crystallinity and lower melting. The HS and HI fractions had similar ethylene content, melting temperatures, crystallinity, and molecular weight

**Table 6. Fractions of Ethylene-1-Hexene Copolymers Made from 8/MAO**

| | fraction | | | |
|---|---|---|---|---|
| | ES[a] | HS[b] | HI[c] | whole polymer |
| % wt | 7 | 37 | 56 | 100 |
| % E | 71 | 86 | 86 | 84 |
| $r_e r_h$ | 0.9 | 2.1 | 2.3 | 2.2 |
| $T_m$ (°C) | 37−51 (45) | 32−111 (42, 99) | 33−110 (43, 98) | 33−111 (43, 98) |
| $\Delta H_f$ (J/g) | 2.0 | 32 | 31 | 29 |
| $M_w$ | 564 000 | 668 000 | 743 000 | 615 000 |
| PDI | 6.9 | 2.2 | 2.2 | 2.5 |

[a] ES = ether soluble. [b] HS = heptane soluble. [c] HI = heptane insoluble.

to the unfractionated polymer. All three fractions were of relatively high molecular weight ($M_w \sim 10^6$) and felt rubbery to the touch.

In general, the molecular weight distributions of the unfractionated polymers and those of the HS and HI fractions were relatively narrow (PDI $\sim$ 2.2−2.5),[42] whereas those of the ES fractions were broader (PDI = 7−8).[42]

## Discussion

Metallocene catalysts have provided new opportunities for the synthesis of ethylene-α-olefin copolymers. These catalysts typically incorporate larger amounts of comonomer than heterogeneous Ti or Cr catalysts and generate copolymers with uniform composition distributions, low polydispersities and random to slightly alternating sequence distributions.[13,43]

The comonomer selectivity of a catalyst is gauged from the copolymerization parameters, which can be determined from the experimentally measured sequence distribution of monomers by $^{13}C$ NMR. The reactivity ratios $r_e$ and $r_c$ (e = ethylene, c = comonomer) are

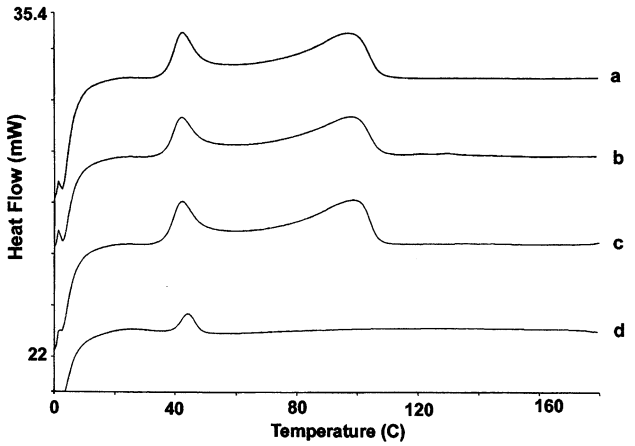


**Figure 6.** DSC heating curves for the fractions of an 84% ethylene EH copolymer made by **8**/MAO (see Table 6): (a) whole polymer; (b) heptane-insoluble fraction; (c) heptane-soluble fraction; (d) ether-soluble fraction.

defined as the ratio of the homopropagation to the cross-propagation rate constants ($r_e = k_{ee}/k_{ec}$, $r_c = k_{cc}/k_{ce}$) of the first-order Markov copolymerization equations.[44] They represent the reactivity of the catalyst toward the two incoming monomers. The product of reactivity ratios $r_e r_c$ gives an indication of the distribution of monomers across the polymer chain. A value of $r_e r_c < 1$ suggests an alternating copolymer structure, $r_e r_c = 1$ indicates a random distribution of comonomers, and $r_e r_c > 1$ suggests the tendency to form blocks of one or both comonomers.

By $^{13}$C NMR, the values of $r_e$ and $r_c$ are calculated from the copolymer triad sequence distributions by the following equations:

$$r_e = \frac{2EEE + EEC}{(2ECE + CCE)X}$$

$$r_c = \frac{(2CCC + CCE)X}{2ECE + CCE}$$

where E is an ethylene unit, C is a comonomer unit, and $X$ is the ratio of mole fractions of ethylene to comonomer in the feed.[45]

The vast majority of metallocene catalysts yield copolymers with random to slightly alternating sequence distributions ($0.2 \leq r_e r_c \leq 1.0$).[13,45] A small subset of stereorigid metallocenes yield copolymers with sequence distributions that deviate from ideal ($r_e r_c = 1.0$); these include highly alternating ($r_e r_c = 0.01-0.005$)[16−19,21−23,25] or slightly blocky ($r_e r_c = 2.0-4.0$) copolymers.[20,24]

**Sequence Distribution.** The sequence distribution of ethylene copolymers is expected to have a significant influence on the physical properties, but there are few systematic studies of these effects due to our limited ability to control the sequence distributions. Our approach to the synthesis of nonrandom copolymers has been to investigate metallocenes that can exhibit multisite behavior, either by exploiting the conformational dynamics of flexible ligand environments or by taking advantage of the multiple coordination sites of unsymmetrical coordination compounds. The latter hypothesis has proven to be a particularly effective strategy for generating highly alternating (and in some cases isotactic) copolymers:[16−19,21−23,25] we have recently shown that certain $C_s$-symmetric catalysts generate highly alternating copolymers by the alternating insertion of ethylene and α-olefins at heterotopic coordination sites that exhibit different kinetic selectivities for the two comonomers.[16,17]

For the synthesis of blocky copolymers, we have investigated conformationally dynamic metallocenes, guided by the hypothesis that different conformational diastereomers should exhibit different selectivities for comonomers and lead to nonideal sequence distributions. Previous studies with bis(2-phenylindenyl)-zirconocene or the mixed-ring metallocene (1-methyl-2-phenylindenyl)(2-phenylindenyl)zirconocene yielded copolymers with sequence distributions very close to ideal ($r_e r_c = 0.84-1.3$).[30,46,47] Model studies of the conformationally constrained syn and anti isomers of these catalysts demonstrated that the comonomer selectivities of the various conformations are different but apparently not sufficiently different to manifest a sequence distribution in the final polymer that deviates significantly from $r_e r_c = 1.0$.[46] In contrast, the sequence distributions of the EP and EH copolymers derived from the 1-benzyl-substituted metallocene **8** yield sequence distributions enriched in EEE and CCC (C = comonomer P or H) homosequences ($r_e r_c = 1.9-2.5$, Tables 3−5). Metallocene **8** produced EP copolymers containing nearly twice as many EEE and PPP sequences as those in copolymers made from **2**, **3**, and **7** at similar compositions (Table 2). This enhancement of EEE and CCC sequences is also manifested in the parameter $r_e r_c$ which is higher for polymers derived from **8** ($r_e r_c = 1.8-2.5$) than for those derived from **1**, **2**, **3**, and **7** ($r_e r_c = 0.5-1.1$).

The presence of the 1-benzyl substituent in **8** appears to be important in generating copolymers with enhanced EEE and CCC homosequences, as metallocene **7** yields copolymers with a more random distribution (Table 2). Moreover, preliminary investigations of analogously substituted mixed-ring metallocenes related to **8** containing 1-methyl, 1-ethyl, 1-isobutyl, and 1-phenethyl substituents yield copolymers with NMR-derived sequence distributions close to ideal ($r_e r_c = 0.88-1.3$).[48]

While we cannot unambiguously establish that the conformational dynamics are responsible for the enhanced homosequences in these copolymers, our current hypothesis is that the conformational dynamics and the presence of the benzyl substituent both play a role in influencing the copolymerization behavior of these metallocenes. Among the conformations likely to be accessible, some should position the benzyl substituent in the vicinity of the active site (as observed in the solid state, Figure 1), whereas other conformations could direct the 1-benzyl substituent away from the active site (Figure 7). For those conformations where the benzyl is directed over the active site, reversible binding of the aryl ring to the cationic center might modulate the copolymerization behavior of this conformation relative to those conformations where the benzyl cannot readily bind to the metal center. The reversible binding of pendant benzyl groups has been observed in other metallocene systems and in some cases leads to catalysts which exhibit unusual polymerization (or trimerization)[49] behavior.[50−52,53−65]

The lower productivities with the benzyl-substituted metallocene **8** are also consistent with this hypothesis: a lower activity and higher ethylene selectivity might be expected if the incoming olefin must first displace

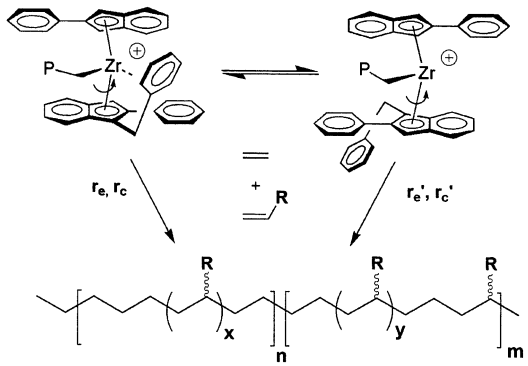


**Figure 7.** Proposed mechanism for generating different comonomer sequences of ethylene-α-olefin copolymer.

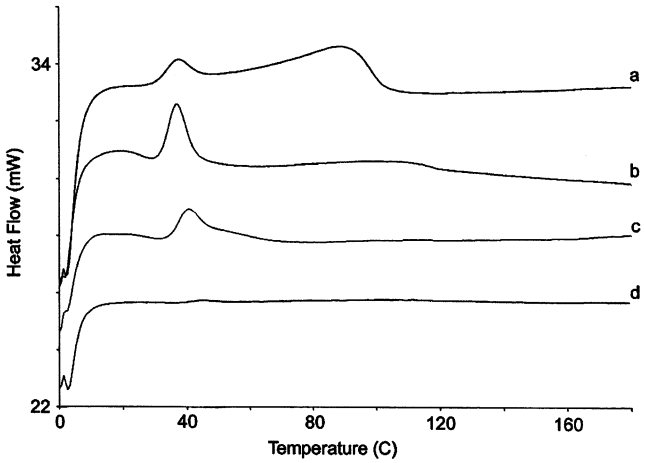


**Figure 8.** DSC heating curves for 80−81% ethylene EH copolymers with different: sequence distributions: (a) $r_e r_h$ = 2.2, %$E$ = 80, $T_m$ = 28−104 (37, 89) °C, $\Delta H_f$ = 18 J/g; (b) $r_e r_h$ = 1.2, %$E$ = 80, $T_m$ = 32−50 (37) °C, $\Delta H_f$ = 4.3 J/g; (c) $r_e r_h$ = 0.63, %$E$ = 81, $T_m$ = 32−70 (41) °C, $\Delta H_f$ = 6.1 J/g; (d) $r_e r_h$ = 0.01, %$E$ = 81, $T_m$ = none, $\Delta H_f$ = none.

the bound benzyl group to coordinate to the metal. Further studies are warranted to assess the role of weak donor ligands on copolymerization behavior.

**Influence of Sequence Distribution on Thermal Properties.** The enrichment of the EEE and CCC sequences in copolymers derived from **8**, as determined by NMR, is also manifested in the melting behavior. Because of the ability of propylene comonomer units to cocrystallize with ethylene, EH copolymers were used to study the relationship between sequence distribution and melting behavior, since it has been established that 1-hexene does not enter the crystal lattice of polyethylene.[4,6,7,66−68] Copolymers derived from **8**/MAO consistently exhibited higher melting points than random copolymers at similar compositions. The melting points of the copolymers as a function of composition (Figures 3 and 4) provided evidence for crystallinity even at 50−60% ethylene composition, suggesting the presence of ethylene sequences that were long enough to crystallize even at relatively low ethylene contents.

The effect of sequence distribution on the melting behavior of ethylene−1-hexene copolymers is further illustrated in Figure 8, which shows the DSC melting curves for a series of EH copolymers of similar composition (80−81% ethylene) with different sequence distributions. The polymers were made using **8**/MAO (**a**), **3**/MAO (**b**), the metallocene [dimethylsilyl(N-*tert*-butylamido)(tetramethylcyclopentadienyl)]titanium dichloride/MAO (**c**), and [dimethylsilyl(4,7-dimethylindenyl)-(fluorenyl)]zirconium dichloride/MAO (**d**). Polymers **a**−**d** had molecular weights ($M_w$) on the order of $10^5$, with the exception of **b** which had a $M_w$ in excess of $1 \times 10^6$.

The highest melting ($T_m$ = 28−104 (37, 89) °C) and most crystalline ($\Delta H_f$ = 18 J/g) polymer had a sequence distribution containing longer ethylene runs (**a**, $r_e r_h$ = 2.2). The polymer with a highly alternating sequence distribution (**d**, $r_e r_h$ = 0.01) did not exhibit any melting behavior. The polymers with random (**b**, $r_e r_h$ = 1.2) or close to random sequence distributions (**c**, $r_e r_h$ = 0.63) had significantly lower melting temperatures (**b**, $T_m$ = 32−50 (37) °C; **c**, $T_m$ = 32−70 (41) °C) and crystallinities (**b**, $\Delta H_f$ = 4.3 J/g; **c**, $\Delta H_f$ = 6.1 J/g).

These results are consistent with that predicted by Flory and Allegra,[8,10] where the smallest and largest melting point depressions at any given composition are observed for copolymers with blocky and alternating sequence distributions, respectively. However, it was observed that even though the sequence distribution of **b** was less alternating than that of **c**, the $T_m$ and $\Delta H_f$ for **b** were lower than those of **c**. This could be the manifestation of an additional melting point depression occurring in random copolymers of higher molecular weight, a phenomenon reported by Mandelkern et al., who had studied the influence of molecular weight on the melting behavior and crystallinity of random copolymers of ethylene and had found that melting temperatures and crystallinity decreased with increasing molecular weight.[5]

Fractionations were carried out to establish that the melting behavior and high $r_e r_c$ values obtained for **8**/MAO were not the result of intermolecular heterogeneity of the chains.[11,12,69] The heptane-soluble (HS) and heptane-insoluble (HI) fractions, which accounted for over 90% of the whole polymer, were virtually indistinguishable by DSC and $^{13}C$ NMR to the whole polymer (Figure 6 and Table 6). Nevertheless, all samples exhibited a small amount (3−8%) of an ether-soluble fraction that consistently had lower amounts of ethylene (70−71%) and a broad molecular weight distribution. The origin of the small 1-hexene-enriched ether-soluble (ES) fraction was investigated by conducting polymerization experiments under conditions that would reduce the decomposition rate of the catalyst. It was observed from the productivities that **8**/MAO decomposed more rapidly at higher temperatures. One sample was made by polymerizing at 2 °C for 20 min, and another sample was obtained by polymerizing at 20 °C for 5 min. The observed decrease in the amount of ether-soluble material present in copolymers made at lower temperatures and at shorter polymerization times suggests that the ES fractions are derived from the decomposition of the catalyst to a species that more readily incorporates 1-hexene. One possible candidate for this decomposition process is the thermal ortho C−H activation of the pendant benzyl group, as has been observed in other benzyl-substituted metallocenes.[70−73]

**Comonomer Incorporation.** The 2-arylindenylmetallocenes **2**, **3**, **7**, and **8** are unusually adept at incorporating comonomer. The relatively low values of $r_e$ and relatively high values of $r_p$ (Tables 2 and 3) reveal that metallocenes **2**, **3**, **7**, and **8** all exhibit a higher selectivity toward comonomer incorporation than the bridged metallocene *rac*-EBIZrCl$_2$, **1**. The trend for reactivity toward propylene in increasing order was **1** < **8** ≪ **2** < **7** < **3**. This is consistent with other studies in our laboratories which show that 2-arylindenyl zirconocenes show an

unusually high tendency to incorporate comonomer in ethylene-α-olefin copolymerizations.[30,34,46] The origin of this high selectivity remains unclear, but we attribute it to the electronic influence of the 2-aryl substituent since this behavior is shared by a number of fluorenyl-ligated zirconocenes and those which contain annulated aromatic ligands.[45,74]

## Conclusions

Conformationally dynamic metallocenes derived from 2-arylindenyl ligands yield copolymers with a range of sequence distributions. The melting behavior of these copolymers depends sensitively on the sequence distribution for a given composition, with the lowest melting points observed for copolymers with alternating sequence distributions and the highest melting points observed for copolymers enriched in EEE and CCC sequences. Copolymers with enhanced monomer homosequences were observed for metallocenes substituted with a 1-benzyl substituent; reversible binding of the pendant 1-benzyl substituent, coupled with the conformational dynamics of the ligand system, may be responsible for this unusual copolymerization behavior.

## Experimental Section

**General Considerations.** All organometallic reactions were conducted under nitrogen, using standard Schlenk and drybox techniques. Elemental analyses were performed by Desert Analytics. NMR spectra were obtained on a 400 MHz Varian XL-400 spectrometer. Unless otherwise specified, all solvents and reagents were purchased commercially and used without further purification. The complexes (2-phenylindenyl)-zirconium trichloride, *rac*-[ethylenebis(1-indenyl)]zirconium dichloride (**1**), and bis(2-phenylindenyl)zirconium dichloride (**2**), were prepared according to literature procedures, and bis-[(3′,5′-di-*tert*-butyl)phenylindenyl]zirconium dichloride (**3**) was obtained from BP Amoco.[29,75] Toluene and pentane were passed through two purification columns packed with activated alumina and copper catalyst, and diethyl ether and tetrahydrofuran were passed through a column of activated alumina. All were collected under nitrogen. Ethylene gas was purchased from Matheson, and liquid propylene was purchased from Scott Specialty Gases. Both monomers were passed through two purification columns packed with activated alumina and copper catalyst. 1-Hexene was purchased from Aldrich and dried over calcium hydride or sodium metal. Methylaluminoxane (MAO) was purchased from Akzo Nobel and dried under vacuum. Unless otherwise indicated, all polymerizations were conducted at 20 °C. GPC analyses of polymers were performed by BP Amoco and DuPont Dow Elastomers.

**Methyl 3,5-Di-*tert*-butylbenzoate (4).** 3,5-Di-*tert*-butylbenzoic acid (2 g, 8.5 mmol) was dissolved in methanol (50 mL). Thionyl chloride (0.94 mL, 13 mmol) was added at 0 °C. The mixture was stirred at room temperature for 16 h, and the solvent was removed under vacuum. The residual white solid was used without purification (1.92 g, 91%).

$^1$H NMR ($CDCl_3$): $\delta$ 1.33 (18H, s), 3.89 (3H, s), 7.60 (1H, m), 7.87 (2H, m).

$^{13}C\{^1H\}$ NMR ($CDCl_3$): $\delta$ 31.35, 34.92, 51.98, 123.76, 127.05, 129.49, 150.99, 167.80.

**2-(3′,5′-Di-*tert*-butyl)phenylindene (5).** Magnesium powder (1.65 g, 68 mmol) was activated with 1,2-dibromoethane (0.366 mL, 4.25 mmol) in THF (15 mL). The solvent was removed under vacuum to remove all volatiles. A solution of *o*-xylylene dichloride (3 g, 17 mmol) dissolved in THF (125 mL) was added dropwise to the activated magnesium at room temperature over 2 h, and the mixture was stirred at room temperature for 16 h. A solution of **4** (2.81 g, 11.3 mmol) in THF (125 mL) was added dropwise to the Grignard solution over 2 h at −78 °C. The mixture was warmed to room temperature and stirred for 16 h. Water was added to quench excess Grignard, and the solution was acidified with hydrochloric acid to pH ∼1. The product was extracted with diethyl ether, dried over $MgSO_4$, and the solvent was removed under vacuum. The solid was dissolved in toluene, *p*-toluenesulfonic acid (0.44 g, 2.6 mmol) was added, and the solution was refluxed for 3 h. The mixture was washed with water, and the water layer was extracted with ether. The organic layers were combined and dried with $MgSO_4$. Solvent was removed under vacuum. The solid residue was purified by flash chromatography using pentane (2.95 g, 85%).

$^1$H NMR ($CDCl_3$): $\delta$ 1.39 (18H, s), 3.84 (2H, s), 7.1−7.5 (7H, m).

$^{13}C\{^1H\}$ NMR ($CDCl_3$): $\delta$ 31.46, 34.89, 39.22, 119.97, 120.78, 122.03, 123.58, 124.48, 126.03, 126.53, 135.23, 143.17, 145.56, 147.55, 150.99.

**1-Benzyl-2-(3′,5′-di-*tert*-butyl)phenylindene (6).** *n*-Butyllithium (6.5 mL, 1.04 mmol, 1.6 M in hexanes) was added via syringe to a solution of **5** (3 g, 9.85 mmol) in THF (150 mL) at 0 °C, and the solution was stirred at room temperature for 2 h. Benzyl bromide (3.57 mL, 30 mmol) was added slowly to the solution, and the mixture was stirred at 40 °C for 24 h. Solvent was removed under vacuum, and methanol was added to the yellowish residue to precipitate the product. The mixture was filtered through a medium glass frit, and a white solid was collected, washed several times with methanol, and then dried under vacuum (0.8 g, 62%).

$^1$H NMR ($CDCl_3$): $\delta$ 1.27 (18H, s), 3.93 (2H, s), 4.18 (2H, s), 7−7.6 (12H, m).

$^{13}C\{^1H\}$ NMR ($CDCl_3$): $\delta$ 31.34, 32.20, 34.81, 41.33, 119.81, 121.29, 122.27, 123.35, 124.57, 125.93, 126.37, 128.19, 128.46, 135.83, 136.07, 139.57, 142.56, 143.94, 146.86, 150.77.

**[2-(3′,5′-Di-*tert*-butyl)phenylindenyl][2-phenylindenyl]-zirconium Dichloride (7).** *n*-Butyllithium (0.8 mL, 1.28 mmol, 1.6 M in hexanes) was added via syringe to a solution of **5** (0.39 g, 1.28 mmol) in diethyl ether at 0 °C, and the solution was stirred at room temperature overnight. The solvent was removed under vacuum, and the yellow powdery (2-phenylindenyl)zirconium trichloride (0.49 g, 1.26 mmol) was added to the solid residue. Toluene (50 mL) was added to the solids, and the reaction was stirred at room temperature for 22 h. After Schlenk filtration through Celite, the solution was concentrated, carefully layered with pentane, and then allowed to sit at room temperature. The crystalline yellow product was isolated by removing the supernatant solution by cannula and then washed several times with pentane (0.138 g, 16%).

$^1$H NMR ($C_6D_6$): $\delta$ 1.42 (18H, s), 6.50 (2H, s), 6.67 (2H, s), 6.9−7.0 (8H, m), 7.10 (1H, t, $J_{HH}$ = 7.2 Hz), 7.21 (2H, t, $J_{HH}$ = 7.6 Hz), 7.50 (2H, d, $J_{HH}$= 7.6 Hz), 7.56 (1H, s), 7.71 (2H, d, $J_{HH}$ = 1.6 Hz).

$^{13}C\{^1H\}$ NMR ($CDCl_3$): $\delta$ 31.81, 35.37, 104.32, 104.82, 121.58, 123.20, 124.93, 126.73, 126.77, 126.96, 127.08, 127.24, 128.92, 128.99, 129.33, 131.36, 132.02, 132.16, 133.52, 151.92.

Anal. Calcd (found) for $C_{45}H_{44}C1_2Zr$: C, 69.49 (69.79); H, 5.83 (5.62).

**[1-Benzyl-2-(3′,5′-di-*tert*-butyl)phenylindenyl][2-phenylindenyl]zirconium Dichloride (8).** *n*-Butyllithium (0.8 mL, 1.27 mmol, 1.6 M in hexanes) was added via syringe to a solution of **6** (0.5 g, 1.27 mmol) in diethyl ether at 0 °C, and the solution was stirred at room temperature for 3 h. The solvent was removed under vacuum, and the yellow powdery (2-phenylindenyl)zirconium trichloride (0.494 g, 1.27 mmol) was added to the solid residue. Toluene (50 mL) was added to the solids, and the reaction was stirred at room temperature for 18 h. The mixture was Schlenk filtered through Celite, and the solvent was removed under vacuum. The product was isolated by adding pentane to the residue and then increasing the solubility of the product by adding a small amount of toluene. The product was isolated as a bright yellow powder. A second crop was isolated from the supernatant solution (0.279 g, 29%).

$^1$H NMR ($C_6D_6$): $\delta$ 1.40 (18H, s), 4.63 (1H, d, $J_{HH}$ = 16.8 Hz), 4.78 (1H, d, $J_{HH}$ = 16.8 Hz), 5.95 (1H, s), 6.25 (1H, d, $J_{HH}$ = 2.2 Hz), 6.56 (1H, d, $J_{HH}$ = 2.2 Hz), 6.8−7.6 (21H, m).

$^{13}C\{^1H\}$ NMR ($CDCl_3$): $\delta$ 31.49, 32.72, 35.00, 100.53, 101.75, 105.09, 122.20, 122.44, 123.64, 124.35, 124.50, 125.00, 125.39, 125.756, 126.04, 126.32, 126.37, 126.50, 126.53, 126.70, 128.07, 128.20, 128.69, 128.83, 132.72, 133.35, 133.83, 139.87, 150.90.

Anal. Calcd (found) for $C_{45}H_{44}Cl_2Zr$: C, 72.36 (72.01); H, 5.94 (6.17).

**Ethylene Polymerization.** In a 300 mL stainless steel Parr reactor, 150 mg of MAO in 98 mL of toluene, was equilibrated for 30 min at 20 °C, with 16 psig of ethylene overhead pressure. A solution of metallocene ($1 \times 10^{-6}$ mol) in toluene (2 mL) was injected into the reactor via ethylene pressure. The polymerization was run for 20 min and then quenched with methanol (10 mL). The polyethylene was precipitated from acidified methanol, filtered, washed with methanol, and dried under vacuum at 40 °C.

**Propylene Polymerization.** In a 300 mL stainless steel Parr reactor, 150 mg of MAO in 8 mL of toluene was equilibrated for 30 min at 20 °C, with 90 mL of liquid propylene. A solution of metallocene ($2.68 \times 10^{-6}$ mol) in toluene (2 mL) was injected into the reactor via argon pressure (250 psig). The polymerization was run for 20 min and then quenched with methanol (10 mL). The polypropylene was precipitated from acidified methanol, filtered, washed with methanol, and dried under vacuum at 40 °C.

**Ethylene—Propylene Copolymerization.** In a 300 mL stainless steel Parr reactor, 100 mg of MAO in 18 mL of toluene was equilibrated for 30 min at 20 °C, with 100 mL of liquid propylene and gaseous ethylene overhead pressure. Metallocene solution ($4 \times 10^{-7}$ mol) in toluene (2 mL) was injected into the reactor via ethylene pressure, and the polymerization was run for 20 min, after which methanol (10 mL) was injected to quench the reaction. The ethylene–propylene copolymer was precipitated from acidified methanol, filtered, washed with methanol, and dried under vacuum at 40 °C.

**Ethylene—1-Hexene Copolymerization.** In a 300 mL stainless steel Parr reactor, 100 mg of MAO in 35 mL 1-hexene was equilibrated for 30 min at 20 °C, with gaseous ethylene overhead pressure. Catalyst solution ($4 \times 10^{-7}$ mol) in toluene/1-hexene (5 mL) was injected into the reactor via ethylene pressure, and the polymerization was run for 20 min, and then quenched with methanol (10 mL). The ethylene-hexene copolymer was precipitated from acidified methanol, filtered, washed with methanol, and dried under vacuum at 40 °C.

**Polymer Characterization.** Polymer molecular weights and molecular weight distributions were determined by high-temperature gel permeation chromatography (GPC) using high-density polyethylene calibration standards. Melting point ranges and heats of fusion were determined by differential scanning calorimetry (DSC) using a Perkin-Elmer DSC-7. All DSC samples were heated to 180 °C, held at that temperature for 10 min, cooled to 20 °C at a rate of 10 °C/min, and then aged at room temperature for 48 h. DSC scans were obtained by heating the samples to 180 °C at a rate of 20 °C/min. The isothermally crystallized samples were prepared and run similarly to what was described in the literature.[39] The samples were heated to 180 °C, held at that temperature for 5 min, and then quenched. The samples were then heated to the desired annealing temperature at a rate of 40 °C/min and held at that temperature for 1 h, after which the samples were quenched. The DSC scans were then obtained at a rate of 10 °C/min. $^{13}C$ NMR measurements were obtained using a Varian Unity Innova 300 MHz instrument for polymer samples (80 mg in 2 mL of *o*-dichlorobenzene/10 vol % benzene-$d_6$ with Cr(acac)$_3$ as a relaxation agent) at 100 °C in 10 mm NMR tubes. The delay time between pulses was set at 5 s.

**Fractionation of Ethylene—1-Hexene Copolymer.** A 1.01 g sample of EH copolymer was transferred into an extraction thimble, plugged with glass wool, capped with filter paper, and placed in a Kumagawa extractor. The fractions were obtained by successive extractions into refluxing ether and then heptane under nitrogen for 24 h each. The ether- and heptane-soluble fractions were isolated by precipitation from methanol and then dried under vacuum together with the heptane-insoluble fraction.

**Acknowledgment.** Financial support from BP Amoco and a Bayer Graduate Fellowship to J.H. are gratefully acknowledged. We thank Dave McFarland (BP Amoco) and Peter Fox (DuPont Dow Elastomers) for high-temperature GPC measurements.

**Supporting Information Available:** Tables of sequence distributions of copolymer samples, pentad distributions of polypropylenes, additional fractionation data, and crystal structure data and text describing the crystal stucture determination (26 pages). This material is free of charge via the Internet at http://pubs.acs.org.

## References and Notes

(1) Scheirs, J.; Kaminsky, W. *Metallocene-based Polyolefins: Preparation, properties, and technology*; John Wiley & Sons Ltd.: Chichester, England, 2000; Vol. 1.
(2) Scheirs, J.; Kaminsky, W. *Metallocene-based Polyolefins: Preparation, properties, and technology*; John Wiley & Sons Ltd.: Chichester, England, 2000; Vol. 2.
(3) Mandelkern, L. In *Crystallization of Polymers*; McGraw-Hill, Inc.: New York, 1964; pp 74−116.
(4) Alamo, R.; Domszy, R.; Mandelkern, L. *J. Phys. Chem.* **1984**, *88*, 6587−6595.
(5) Alamo, R. G.; Chan, E. K. M.; Mandelkern, L. *Macromolecules* **1992**, *25*, 6381−6394.
(6) Alamo, R. G.; Viers, B. D.; Mandelkern, L. *Macromolecules* **1993**, *26*, 5740−5747.
(7) Alamo, R. G.; Mandelkern, L. *Thermochim. Acta* **1994**, *238*, 155−201.
(8) Allegra, G.; Marchessault, R. H.; Bloembergen, S. *J. Polym. Sci., Part B: Polym. Phys.* **1992**, *30*, 809−815.
(9) Ke, B. *J. Polym. Sci.* **1962**, *61*, 47−59.
(10) Flory, P. J. *Principles of Polymer Chemistry*; Cornell University Press: Ithaca, NY, 1953.
(11) Cozewith, C.; Ver Strate, G. *Macromolecules* **1971**, *4*, 482−489.
(12) Cozewith, C. *Macromolecules* **1987**, *20*, 1237−1244.
(13) Galimberti, M.; Piemontesi, F.; Fusco, O. In *Metallocene-Based Polyolefins*; Scheirs, J., Kaminsky, W., Eds.; Wiley: Chichester, England, 2000; Vol. 1; pp 309−343.
(14) Matsugi, T.; Matsui, S.; Kojoh, S.; Takagi, Y.; Inoue, Y.; Nakano, T.; Fujita, T.; Kashiwa, N. *Macromolecules* **2002**, *35*, 4880−4887.
(15) Turner, H. W.; Hlatky, G. G.; Yang, W. H.; Gadkari, A. C.; Licciardi, G. F. U.S. Patent 5,391,629, 1995.
(16) Choo, T. N.; Waymouth, R. M. *J. Am. Chem. Soc.* **2002**, *124*, 4188−4189.
(17) Fan, W.-H.; Leclerc, M. K.; Waymouth, R. M. J. *Am. Chem. Soc.* **2001**, *123*, 9555.
(18) Kaminsky, W.; Beulich, I.; Arndt-Rosenau, M. *Macromol. Symp.* **2001**, *173*, 221−225.
(19) Uozumi, T.; Ahn, C. H.; Tomisaka, M.; Jin, J.; Tian, G.; Sano, T.; Soga, K. *Macromol. Chem. Phys.* **2000**, *201*, 1748−1752.
(20) Galimberti, M.; Piemontesi, F.; Mascellani, N.; Camurati, I.; Fusco, O.; Destro, M. *Macromolecules* **1999**, *32*, 7968−7976.
(21) Arndt, M.; Kaminsky, W.; Schauwienold, A.-M.; Weingarten, U. *Macromol. Chem. Phys.* **1998**, 199.
(22) Jin, J. H.; Uozumi, T.; Sano, T.; Teranishi, T.; Soga, K.; Shiono, T. *Macromol. Rapid Commun.* **1998**, *19*, 337−339.
(23) Leclerc, M. K.; Waymouth, R. M. *Angew. Chem., Int. Ed. Engl.* **1998**, *37*, 922−925.
(24) Galimberti, M.; Piemontesi, F.; Fusco, O.; Camurati, I.; Destro, M. *Macromolecules* **1998**, *31*, 3409−3416.
(25) Uozumi, T.; Miyazawa, K.; Sano, T.; Soga, K. *Macromol. Rapid Commun.* **1997**, *18*, 883−889.
(26) Tagge, C. D.; Kravchenko, R. L.; Lal, T. K.; Waymouth, R. M. *Organometallics* **1999**, *18*, 380−388.
(27) Coates, G. W.; Waymouth, R. M. *Science* **1995**, *267*, 217−219.
(28) Propylene homopolymerizations: **2**, productivity = 2480 kg/mol Zr·hr, [*mmmm*] = 28%, $M_w$ = 459 000, PDI = 3.7; **3**, productivity = 1950 kg/mol Zr·hr, [*mmmm*] = 80%; **7**, productivity = 1310 kg/mol Zr·hr, [*mmmm*] = 34%, $M_w$ = 370 000, PDI = 2.8; **8**, productivity = 310 kg/mol Zr·hr, [*mmmm*] = 24%, $M_w$ = 73 100, PDI = 2.9. Ethylene homopolymerizations: **8**, productivity = 3450 kg/mol Zr·hr, $M_w$ = 780 000, PDI = 4.6.
(29) Wilmes, G.; Lin, S.; Waymouth, R. M. *Macromolecules* **2002**, *35*, 5382−5387.

(30) Kravchenko, R.; Waymouth, R. M. *Macromolecules* **1998**, *31*, 1−6.
(31) Kakugo, M.; Naito, Y.; Mizunuma, K.; Miyatake, T. *Macromolecules* **1982**, *15*, 1150−1152.
(32) Hsieh, E. T.; Randall, J. C. *Macromolecules* **1982**, *15*, 1402−1406.
(33) Randall, J. C. *J. Macromol. Sci.—Rev. Macromol. Chem. Phys.* **1989**, *C29*, 201−317.
(34) Reybuck, S. E.; Meyer, A.; Waymouth, R. M. *Macromolecules* **2002**, *35*, 637−643.
(35) Lehtinen, C.; Lofgren, B. *Eur. Polym. J.* **1997**, *33*, 115−120.
(36) Chien, J. C. W.; He, D. *J. Polym. Sci., Part A: Polym. Chem.* **1991**, *29*, 1585−1593.
(37) Drogemuller, H.; Heiland, K.; Kaminsky, W. *Transition Metals and Organometallics as Catalysts for Olefin Polymerization*; Springer-Verlag: Berlin, 1988; p 303.
(38) Zambelli, A.; Grassi, A.; Galimberti, M.; Mazzocchi, R.; Piemontesi, F. *Makromol. Chem., Rapid Commun.* **1991**, *12*, 523−528.
(39) Minick, J.; Moet, A.; Hiltner, A.; Baer, E.; Chum, S. P. *J. Appl. Polym. Sci.* **1995**, *58*, 1371−1384.
(40) Bensason, S.; Minick, J.; Moet, A.; Chum, S.; Hiltner, A.; Baer, E. *J. Polym. Sci., Part B: Polym. Phys.* **1996**, *34*, 1301−1315.
(41) Alizadeh, A.; Richardson, L.; Xu, J.; McCartney, S.; Marand, H.; Cheung, Y. W.; Chum, S. *Macromolecules* **1999**, *32*, 6221−6235.
(42) GPC Analysis conducted at DuPont Dow Elastomers.
(43) Benedikt, G. M.; Goodall, B. L. *Metallocene-Catalyzed Polymers: Materials, Properties, Processing, and Markets*; Plastics Design Library: Norwich, NY, 1998.
(44) Odian, G. *Principles of Polymerization*; John Wiley & Sons: New York, 1991.
(45) Fink, G.; Richter, W. J. In *Polymer Handbook*, 4th ed.; Brandup, J., Immergut, E. H., Grulke, E. A., Eds.; John Wiley & Sons: New York, 1999; Vol. II; pp 329−337.
(46) Dankova, M.; Kravchenko, R. L.; Cole, A. P.; Waymouth, R. M. *Macromolecules* **2002**, *35*, 2882−2891.
(47) Petoff, J. L. M. Ph.D. Thesis, Stanford University, 1999.
(48) Hung, J.; Kravchenko, R. L.; Petoff, J. L. M.; Waymouth, R. M. Manuscript in preparation.
(49) Deckers, P. J. W.; Hessen, B.; Teuben, J. H. *Angew. Chem., Int. Ed. Engl.* **2001**, *40*, 2516−2519.
(50) Sassmannshausen, J.; Powell, A. K.; Anson, C. E.; Wocadlo, S.; Bochmann, M. *J. Organomet. Chem.* **1999**, *592*, 84−94.
(51) Bochmann, M.; Green, M. L. H.; Powell, A. K.; Sassmannshausen, J.; Triller, M. U.; Wocadlo, S. *J. Chem. Soc., Dalton Trans.* **1999**, 43−49.
(52) Lancaster, S. J.; Robinson, O. B.; Bochmann, M. *Organometallics* **1995**, *14*, 2456−2462.
(53) Bühl, M.; Sassmannshausen, J. *J. Chem. Soc., Dalton Trans.* **2001**, 79−84.
(54) Sassmannshausen, J. *Organometallics* **2000**, *19*, 482−489.
(55) Green, M. L. H.; Sassmannshausen, J. *Chem. Commun.* **1999**, 115−116.
(56) Longo, P.; Amrnendola, A. G.; Fortunato, E.; Boccia, A. C.; Zambelli, A. *Macromol. Rapid Commun.* **2001**, *22*, 339−344.
(57) Schwecke, C.; Kaminsky, W. *J. Polym. Sci., Part A: Polym. Chem.* **2001**, *39*, 2805−2812.
(58) Gillis, D. J.; Tudoret, M.-J.; Baird, M. C. *J. Am. Chem. Soc.* **1993**, *115*, 2543−2545.
(59) Flores, J. C.; Wood, J. S.; Chien, J. C. W.; Rausch, M. D. *Organometallics* **1996**, *15*, 4944−4950.
(60) Gillis, D. J.; Quyoum, R.; Tudoret, M.-J.; Wang, Q.; Jeremic, D.; Roszak, A. W.; Baird, M. C. *Organometallics* **1996**, *15*, 3600−3605.
(61) Pellechia, C.; Immirzi, A.; Pappalardo, D.; Peluso, A. *Organometallics* **1994**, *13*, 3773−3775.
(62) Zimmermann, K. H.; Pilato, R. S.; Horváth, I. T.; Okuda, J. *Organometallics* **1992**, *11*, 3935−3937.
(63) Licht, E. H.; Alt, H. G.; Milius, W.; Abu-Orabi, S. *J. Organomet. Chem.* **1998**, *560*, 69−75.
(64) Djakovitch, L.; Herrmann, W. A. *J. Organomet. Chem.* **1998**, *562*, 71−78.
(65) Okuda, J.; Zimmermann, K. H. *Chem. Ber.* **1992**, *125*, 637−641.
(66) Richardson, M. J.; Flory, P. J.; Jackson, J. B. *Polymer* **1963**, *4*, 221−236.
(67) Perez, E.; Vanderhart, D. L.; Crist, B., Jr.; Howard, P. R. *Macromolecules* **1987**, *20*, 78−87.
(68) Laupretre, F.; Monnerie, L.; Barthelemy, L.; Wairon, J. P.; Sanzean, A.; Roussel, D. *Polym. Bull. (Berlin)* **1986**, *15*, 159−164.
(69) Floyd, S. *J. Appl. Polym. Sci.* **1987**, *34*, 2559−2574.
(70) Licht, E. H.; Alt, H. G.; Karim, M. M. *J. Organomet. Chem.* **2000**, *599*, 261−274.
(71) Djakovitch, L.; Herrmann, W. A. *J. Organomet. Chem.* **1997**, *545−546*, *399−405*.
(72) Erker, G.; Mühlenbernd, T. *J. Organomet. Chem.* **1987**, *319*, 201−211.
(73) Bulls, A. R.; Bercaw, J. E.; Manriquez, J. M.; Thompson, M. E. *Polyhedron* **1988**, *7*, 1409−1428.
(74) Schneider, M. J.; Suhm, J.; Mulhaupt, R.; Prosenc, M. H.; Brintzinger, H. H. *Macromolecules* **1997**, *30*, 3164−3168.
(75) Waymouth, R. M.; Bendig, L. L.; Moore, E. J.; Myers, C. L.; Quan, R. W.; Ernst, A. B. US Patent 6,160,064, 2000.

MA021779V